Journal of Pathology
J Pathol 2009; **217**: 420–430
Published online 9 October 2008 in Wiley InterScience
(www.interscience.wiley.com) **DOI:** 10.1002/path.2466

Original Paper

A20 deletion is associated with copy number gain at the *TNFA/B/C* locus and occurs preferentially in translocation-negative MALT lymphoma of the ocular adnexa and salivary glands

E Chanudet,[1] H Ye,[1] J Ferry,[2] CM Bacon,[1] P Adam,[3] HK Müller-Hermelink,[3] J Radford,[4] SA Pileri,[5] K Ichimura,[1] VP Collins,[1] RA Hamoudi,[1] AG Nicholson,[6] AC Wotherspoon,[7] PG Isaacson[8] and MQ Du[1]*

[1] *Division of Molecular Histopathology, Department of Pathology, University of Cambridge, UK*
[2] *Department of Pathology, Massachusetts General Hospital, Boston, MA, USA*
[3] *Institute of Pathology, University of Würzburg, Germany*
[4] *Cancer Research UK, Department of Medical Oncology, Christie Hospital, Manchester, UK*
[5] *Unità Operativa di Emolinfopatologia, Università degli Studi di Bologna, Italy*
[6] *Department of Histopathology, Royal Brompton Hospital, London, UK*
[7] *Department of Histopathology, Royal Marsden Hospital, London, UK*
[8] *Department of Histopathology, University College London, UK*

**Correspondence to:*
MQ Du, Division of Molecular Histopathology, Department of Pathology, University of Cambridge, Box 231, Level 3, Lab Block, Addenbrooke's Hospital, Hills Road, Cambridge CB2 OQQ, UK.
E-mail: mqd20@cam.ac.uk

No conflicts of interest were declared.

Received: 21 July 2008
Revised: 28 August 2008
Accepted: 24 September 2008

Abstract

The genetic basis of MALT lymphoma is largely unknown. Characteristic chromosomal translocations are frequently associated with gastric and pulmonary cases, but are rare at other sites. We compared the genetic profiles of 33 ocular adnexal and 25 pulmonary MALT lymphomas by 1 Mb array–comparative genomic hybridization (CGH) and revealed recurrent 6q23 losses and 6p21.2–6p22.1 gains exclusive to ocular cases. High-resolution chromosome 6 tile-path array–CGH identified NF-κB inhibitor *A20* as the target of 6q23.3 deletion and *TNFA/B/C* locus as a putative target of 6p21.2–22.1 gain. Interphase fluorescence *in situ* hybridization showed that *A20* deletion occurred in MALT lymphoma of the ocular adnexa (8/42 = 19%), salivary gland (2/24 = 8%), thyroid (1/9 = 11%) and liver (1/2), but not in the lung (26), stomach (45) and skin (13). Homozygous deletion was observed in three cases. *A20* deletion and *TNFA/B/C* gain were significantly associated ($p < 0.001$) and exclusively found in cases without characteristic translocation. In ocular cases, *A20* deletion was associated with concurrent involvement of different adnexal tissues or extraocular sites at diagnosis ($p = 0.007$), a higher proportion of relapse (67% versus 37%) and a shorter relapse-free survival ($p = 0.033$). *A20* deletion and gain at *TNFA/B/C* locus may thus play an important role in the development of translocation-negative MALT lymphoma.

Keywords: ***A20*; TNF; MALT lymphoma; array comparative genomic hybridization**

Introduction

Extranodal marginal zone B cell lymphoma of mucosa-associated lymphoid tissue (MALT lymphoma) arises in the acquired MALT resulting from chronic inflammatory or autoimmune disorders. MALT lymphomas of the stomach, skin and ocular adnexa are linked, although to variable degrees, to infection with *Helicobacter pylori, Borrelia burgdorferi* and *Chlamydia psittaci*, respectively, while those of the salivary gland and thyroid are closely associated with the autoimmune disorders lymphoepithelial sialadenitis and Hashimoto thyroiditis, respectively [1].

The acquisition of genetic abnormalities plays a critical role in the development of MALT lymphoma [1]. Four recurrent chromosomal translocations occur at markedly variable frequencies in MALT lymphoma of different sites. t(11;18)(q21;q21)/*API2–MALT1* occurs frequently in the lung (40%), stomach (25%) and ocular adnexa (~10%) [2]. t(1;14)(p22;q32)/*BCL10–IGH,* t(14;18)(q32;q21)/*IGH–MALT1* and t(3;14)(p13;q32)/*FOXP1–IGH*, are relatively infrequent, t(1;14) and t(14;18) occurring mostly in the lung (6–7%) and t(3;14) in the stomach (4%) [3–6]. While the role of the early B cell development regulator FOXP1 in lymphoma remains unclear [7], chromosomal translocations involving BCL10 or MALT1 exert their oncogenic activities through the constitutive activation of NF-κB [8], leading to the expression of a

number of genes involved in cell survival and proliferation. Importantly, gastric MALT lymphomas harbouring t(11;18)(q21;q21)/*API2–MALT1* do not respond to *H. pylori* eradication, underlying the importance of detecting these translocations in clinical management [9,10].

The majority of MALT lymphomas are negative for these chromosomal translocations and their molecular genetics is poorly understood. Several trisomies are frequently associated with MALT lymphoma [11,12], particularly those without t(11;18)(q21;q21). Our previous study of translocation-negative MALT lymphomas of the stomach and salivary glands by metaphase comparative genomic hybridization (CGH) showed recurrent trisomies (3/12/18) and discrete gains at 9q34, 11q11–13 and 18q21 [13,14]. Interestingly, these regions contain a number of genes encoding positive regulators of the NF-κB pathway, such as CARD9, TRAF2, RELA and MALT1. To address whether MALT lymphomas of other sites show common or distinct genetic alterations, we investigated the genomic profiles of ocular and pulmonary MALT lymphomas by array–CGH, and characterized novel abnormalities by interphase florescence *in situ* hybridization (FISH) in MALT lymphomas of various sites.

Methods

Tissue specimens

Archival formalin-fixed paraffin-embedded tissue (FFPE) biopsies from primary MALT lymphomas were used for genomic profiling (ocular adnexa, 46 cases; lung, 31 cases) and FISH investigation (various anatomical sites, 185 cases). Local ethical guidelines were followed for the use of archival tissues for research with the approval of the ethics committees of the institutions involved.

DNA preparation

Tumour cells were microdissected from haematoxylin-stained slides and digested with proteinase K [15]. DNA was purified using phenol–chloroform or QIAamp DNA Micro Kit (QIAGEN, Crawley, UK) and quantified by Picogreen™ (Molecular Probes, Eugene, OR, USA). DNA quality was assessed by amplification of variously sized gene fragments [16]: only cases with adequate DNA quantity and successful amplification of 200 bp (19% cases) or larger product (81% cases) were used for array–CGH.

Infectious agents and translocation status

Newly retrieved ocular adnexal MALT lymphoma cases from Massachusetts General Hospital, Boston, USA (cases 1–24, Table 2), were screened for *Chlamydia psittaci* (CPS), *C. trachomatis* (CTR) and *C. pneumoniae* (CPN) by PCR and for translocations t(11;18)(q21;q21), t(1;14)(p22;q32), t(14;18)(q32;q21) and t(3;14) (p13;q32) by interphase FISH, as previously described [16,17], while data for the remaining cases were available from previous studies [2,4,] [16,17,18].

Array–CGH

Genomic profiles were obtained using in-house 1 Mb resolution genomic arrays containing 3038 BAC clones in duplicate [15,19]. Briefly, 400 ng tumour and reference DNA were labelled with Cy5 and Cy3, respectively, using a Bioprime labelling kit (Invitrogen, Carlsbad, CA, USA). Array hybridization was carried out for 48 h. Slides were scanned using an Axon 4100A scanner (Molecular Devices, Sunnyvale, CA, USA), images quantified using GenePix Pro 5.1 software (Molecular Devices) and primary data analysed using Microsoft Excel [19]. Genomic changes were identified by an integrated approach combining visual inspection and statistical analysis, with the mean ± 3.2 SD ($\log_2$ value ± 0.20) from normal male/female hybridization used as the threshold value, as previously optimized for FFPE tissues [15]. Genomic changes were ascertained by an adaptive threshold (3–5.5 median absolute deviation) determined from a hidden Markov model to take into account intra- and intersample variations (RH, EC, MQD, manuscript in preparation). Regions showing recurrent copy number changes were searched for potential targeted genes (http://www.ensembl.org/Homo_sapiens).

High-resolution chromosome 6 tile-path array–CGH was performed similarly, using an in-house array containing 1780 BAC/PAC clones in duplicate [20].

Interphase FISH

BAC clones bPG296P20 (*TNFA/B/C* locus, 6p21) and RP11-356i2 (*A20* locus, 6q23), were labelled with spectrum orange and spectrum green, respectively, by nick translation (Abbott Laboratories, Maidenhead, UK). Following confirmation of specificity by FISH on metaphase spreads, the labelled probes were pooled with the chromosome 6 centromere probe CEP6 aqua (Abbott Laboratories) and interphase FISH on FFPE tissue sections was performed as described previously [2]. Image acquisition and processing was performed using a fluorescent microscope (Olympus, BX61, Tokyo, Japan) and Cytovision software (version $2 \cdot 75$; Applied Imaging International, Newcastle, UK). The three-colour FISH assay was validated using cases with and without genetic changes identified by chromosome 6 tile-path array–CGH. The mean + 3SD of false-positive signals in 100 nuclei from three reactive tonsils and three MALT lymphomas without chromosome 6 abnormality by tile-path array–CGH was used as the cut-off value for the diagnosis of aberrations.

Statistical analysis

Correlations between array–CGH/FISH results and clinical parameters were performed using Fisher's

exact test ('stats Package' in R version 2.5.1). The probability of lymphoma relapse-free survival was calculated by the Kaplan–Meier method, with log-rank test for comparison (Statistical Package for Social Sciences version 13, Woking, UK).

Results

1 Mb genomic profile of pulmonary MALT lymphoma

Twenty-five pulmonary MALT lymphomas were successfully analysed by 1 Mb array–CGH. Nine cases had t(11;18)(q21;q21), 2 had t(1;14)(p22;q32) and 14 were negative for the four MALT lymphoma-associated translocations. Overall, chromosomal gains were more frequent than losses (Figure 1a). Trisomies were exclusively found in t(11;18)(q21;q21)-negative cases, including t(1;14)(p22;q32)-positive cases (Table 1). Trisomies 3, 12 and 18 were seen in four, two and three cases, respectively, and concurrent in two cases (Table 1).

Recurrent small discrete gains were found mainly at 8q24 (68%), 9q34 (68%) and 11q12–q13 (36%). They were frequently concurrent, with 16/25 cases showing gain at two of the three loci. Discrete deletions were mainly observed at 9q33 (12%) and 14q32 (12%) (Figure 1a). There was no significant difference in the frequencies of discrete gains and losses between cases with and without t(11;18)(q21;q21) (Table 1).

1 Mb genomic profile of ocular adnexal MALT lymphoma

Thirty-three ocular adnexal MALT lymphomas were successfully investigated by 1 Mb array–CGH. The vast majority (30/33) were negative for the four MALT-lymphoma-associated translocations. Their genomic profiles showed several similarities to pulmonary MALT lymphoma. First, trisomies 3, 12 and 18, often concurrent, were frequent and restricted to t(11;18)-negative cases, including the t(1;14)(p22;q32)-positive case. Second, discrete gains were more frequent than losses, and mainly found at 8q24 (67%), 9q34 (48%) and 11q12–q13 (18%) (Table 2; Figure 1a).

However, unlike pulmonary cases, ocular adnexal MALT lymphoma further showed alterations in chromosome 6 (Figure 1a). Gain of chromosome 6 was found in eight cases (18%), including trisomy 6 (1/8), and gain of whole or a major part of the p arm (6/8) or 6p21–22 (1/8) (Table 2). Interestingly, 6p gain was significantly associated with trisomy 3 (Table 2). Loss of 6q was seen in four cases with a minimum common region (MCR) of deletion involving a single BAC clone (RP11-95M15). Concurrent gain of chromosome 6/6p and loss of 6q23 was observed in two cases (Table 2).

Characterization of chromosome 6 abnormalities by high-resolution chromosome 6 tile-path array–CGH

This manuscript focused on the novel chromosome 6 abnormalities in ocular adnexal MALT lymphoma. Chromosome 6 tile-path array–CGH was performed on eight ocular adnexal cases showing chromosome 6 alterations by 1 Mb array–CGH, and nine cases from the ocular adnexa (7) and lung (2) without evidence of chromosome 6 changes. All chromosome 6 copy number changes identified by 1 Mb array–CGH were confirmed by tile-path array–CGH (Figure 1b).

Of the four cases with 6q deletion, tile-path array–CGH revealed a MCR spanning 1226 kb (137.2–138.4 Mb) at 6q23.3 (Figure 1b). Homozygous deletion was seen in one case that also had trisomy 6, while deletion was hemizygous in three cases. The MCR of deletion harboured six genes, including interleukin 22 receptor $\alpha 2$ (*IL22RA2*), interferon-γ receptor 1 (*IFNGR1*) and TNF-induced protein 3 (TNFAIP3, also known as *A20*) (Figure 1b). Statistical analysis among 6q-deleted cases showed a 603 kb region (137.6–138.2 Mb) consistently within the lowest $\log_2$ value in each case and this region contained only *A20*, a potent inhibitor of NF-κB signalling [21,22].

Tile-path array–CGH identified gain at 6p21 in two additional cases without unequivocal 1 Mb array–CGH evidence of a 6p gain, and defined a restricted MCR of gain of 8.2 Mb at 6p21.2–6p22.1. Four cases further showed a recurrent focal peak (3–6 copies) within the MCR, centred at BAC clone bPG296p20 (6p21.33) (Figure 1b). A search of the 15 genes in this BAC clone and its vicinity revealed *NFκBIL1* (NF-κB inhibitor-like 1), *TNF* (also known as *TNFA*), lymphotoxin α (*LTA* or *TNFB*) and lymphotoxin β (*LTB* or *TNFC*) as putative targets.

Characterization of chromosome 6 abnormalities by FISH

Our FISH assay, simultaneously detecting *A20*, *TNFA/B/C* and chromosome 6 centromere loci, confirmed all the alterations identified by array–CGH and was successfully applied to 166 MALT lymphomas from various sites (Figure 2a–d).

Interphase FISH confirmed gain of extra copies (1–3) of the *TNFA/B/C* locus with or without gain of extra centromere probe signals (Table 3). Gain was frequent in MALT lymphomas of the ocular adnexa ($11/42 = 26\%$) and salivary glands ($5/24 = 21\%$), but was rare or absent in those of the lung, stomach and skin (Figure 2e).

A20 deletion was found exclusively in MALT lymphoma of the ocular adnexa ($8/42 = 19\%$), salivary glands ($2/24 = 8\%$), thyroid ($1/9 = 11\%$) and liver (1/2) (Figure 2e). *A20* homozygous deletion was seen in 3/12 cases (Figure 2d). Interestingly, there was a significant association between *A20* deletion and *TNFA/B/C* locus gain ($p < 0.001$; Figure 2f).

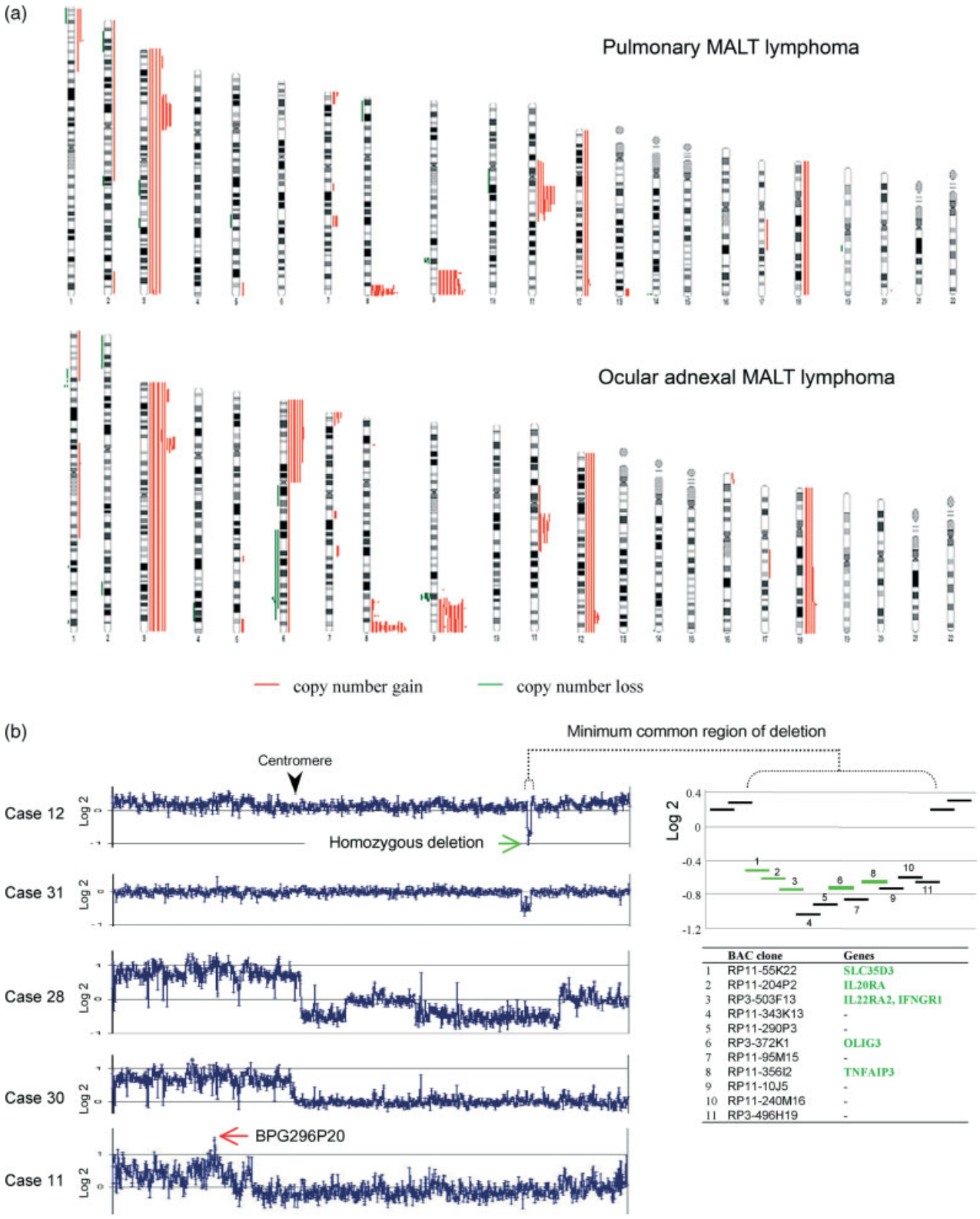

Figure 1. Genomic profiles of MALT lymphoma by array-comparative genomic hybridization. (a) 1 Mb resolution array–CGH profiles of 25 pulmonary and 33 ocular adnexal MALT lymphomas. (b) Characterization of chromosome 6 abnormalities in ocular adnexal MALT lymphoma by high-resolution tile-path chromosome 6 array–CGH. Log_2-transformed normalized Cy5 : Cy3 intensity ratios were plotted against clone position (arranged in genomic order from pter on the left to qter on the right). Cases 12, 31 and 28: examples of 6q deletion with a MCR of 1226 kb at 6q23.3 spanning 11 overlapping BAC clones containing six genes (*SLC35D3*, solute carrier family 35 member D3; *IL20RA*, interleukin 20 receptor α; *IL22RA2*, interleukin 22 receptor α; *IFNGR1*, interferon-γ receptor 1; *OLIG3*, oligodendrocyte transcription factor 3; *TNFAIP3*, tumour necrosis factor-α-induced protein 3, also known as *A20*). Cases 28, 30 and 11: examples of partial tetrasomy 6, involving a whole or major part of 6p. Case 11 shows a focal peak centred at BAC clone bPG296p20, which contains the *TNFA/B/C* locus (6p21.33). Case 12 shows trisomy 6 and 6q23 homozygous deletion, while case 28 displays partial tetrasomy 6 and 6q hemizygous deletion

Table 1. Chromosomal gains and losses in pulmonary MALT lymphomas identified by 1 Mb array–CGH analysis

Case	Translocation	Infectious agents and autoimmune disease	Chromosomal changes[a]	
			Gains	Losses
1	t(11;18)	CPN, CTR	None	None
2	t(11;18)	None	8q24, 9q34, 11p11–q13	9q33
3	t(11;18)	None	8q24, 11q12–13	None
4	t(11;18)	None	None	14q32
5	t(11;18)	Haemolytic anaemia	8q24, 9q34	None
6	t(11;18)	CTR	3p14–21, 8q24, 9q34, 11q12–13	None
7	t(11;18)	CTR	1p32–36, 2q35–37, 3p25, 3p14–21, 7p22, 8q24, 9q34, 11q12–13, 13q34	None
8	t(11;18)	CTR	3p21, 8q24	None
9	t(11;18)	None	8q24, 9q34	None
10	t(1;14)	CTR	1p35, 3, 7p22, 7q22, 8q24, 9q34, 11p11–q13, 12, 18	9q33
11	t(1;14)	None	3, 8q24, 9q34, 12, 18	8p22–23
12	None	CPS	2p25–q22, 3, 8q24, 9q34, 17q12–21	2q22
13	None	CTR	1p35–36, 7p22, 8q24, 9q34, 11p11–q13	9q33
14	None	None	12q24	1p36, 2p24–25, 3q13, 3q22–23, 5q23, 10q11–21, 14q32
15	None	CPN	None	None
16	None	None	7q11, 9q34	14q32
17	None	None	3p21, 5q35, 8q24, 9q34, 20q13	19q13
18	None	Chronic bronchitis	3p21, 7q22, 9q34	None
19	None	CPS	3, 8q24, 9q34, 18	None
20	None	CTR, chronic bronchitis	8q24, 9q34, 11q12–13	None
21	None	None	8q24, 9q34, 13q34	None
22	None	None	3p14–21, 7p22, 7q22, 8q24, 9q34, 11q12–13, 13q34	None
23	None	None	None	None
24	None	CPN	8q24, 9q34, 11q12–13	None
25	None	CPN	None	None

[a] Single BAC clone changes were included only if they were confirmed by tile-path array or fluorescence *in situ* hybridization.
CPS, *Chlamydia psittaci*; CTR, *C. trachomatis*; CPN, *C. pneumoniae*.

Both *A20* deletion and *TNFA/B/C* gain were significantly associated with translocation-negative MALT lymphomas ($p = 0.002$ and $p < 0.001$, respectively). With the exception of one case, No. 13, FOXP1/unknown partner, and a further case, No. 16, t(14;18)(q32;q21)/*IGH–BCL2* [24], all other cases with chromosome 6 abnormalities were negative for MALT lymphoma-associated translocations (Table 3), while 44% of the cases without chromosome 6 abnormalities had a translocation. There was no significant correlation between *TNFA/B/C* locus gain or *A20* deletion and the pattern of expression of BCL10 and MALT1 protein by immunohistochemistry.

Clinicopathological correlations

Unless otherwise stated, clinicopathological correlations were assessed in ocular adnexal MALT lymphoma, for which a sufficient number of cases with adequate clinical data were available (Table 3). Most of the patients were treated by radiotherapy, with a follow-up period of 6–242 months (median 64 months). *A20* deletion was significantly associated with the involvement of the orbital soft tissue by lymphoma at diagnosis ($p = 0.027$) and with concurrent involvement of different adnexal tissues or distant spread at diagnosis ($p = 0.007$) (see Supporting information, Table S1). *A20* deletion was also significantly associated with a shorter lymphoma relapse-free survival ($p = 0.033$; Figure 3a). Lymphoma relapse was more frequent (4/6, 67%) and occurred much earlier (median 11 months) in the cases with *A20* deletion than in those lacking the deletion (6/16 cases, 37.5%; median 51.5 months).

Trisomy 12 was significantly associated with lymphoma relapse ($p = 0.047$), being found in three of nine relapsed cases, which involved distant lymph nodes in two cases and the lip in the remaining case, but in none of the 14 cases without relapse. Trisomy 12 was also significantly associated with a shorter lymphoma relapse-free survival (median 10 months versus 51.5 months without trisomy 12; $p < 0.001$; Figure 3b). Among the three cases with trisomy 12 showing lymphoma relapse, one had *A20* deletion, one showed concurrent trisomies 3 and 18, and the remaining case did not harbour any of these abnormalities. Interestingly, the case with concurrent *A20* deletion and trisomy 12 showed repeated lymphoma

Table 2. Chromosomal gains and losses in ocular adnexal MALT lymphomas identified by 1 Mb array–CGH analysis

Case	Anatomical location	Translocation	Infectious agents[a] and autoimmune disease	Chromosomal changes[b,c]	
				Gains	Losses
1	Conjunctiva	t(11;18)	CPS	7p22, 8q24, 9q34	9q33
2	Orbital soft tissue	t(1;14)	None	3, 8q24, 9q33–34, 12	9q33
3	Orbital soft tissue	*FOXP1* and unknown partner	None	6p21–22, 8q24, 9q33–34, 11q12–13, 18q21	None
4	Orbital soft tissue	None	None	3, 8q24, 9q34, 12, 18	9q33
5	Orbital soft tissue	None	None	3, 6p, 8q24, 9q32–34, 11p11–q13	None
6	Conjunctiva	None	None	7q11, 9q33–34	9q33
7	Orbital soft tissue	None	None	12q24	1p32–34
8	Lachrymal glands, orbital soft tissue	None	None	3p25, 3p21, 8q24, 9q33–34, 12	2q33–34
9	Orbital soft tissue	None	None	7q11, 7q22, 8q24, 16p13	None
10	Orbital soft tissue	None	None	8q24	None
11	Orbital soft tissue	None	None	3, 6p21–25, 8q24	None
12	Conjunctiva., lachrymal glands, orbital soft tissue	None	Ulcerative colitis	3, 6, 8q24, 18	6q23
13	Conjunctiva, orbital soft tissue	None	None	3p25, 3p21, 8q24	6q16–25, 14q32
14	Orbital soft tissue	None	None	3, 8q24, 9q33–34, 17q12–21	None
15	Orbital soft tissue	None	None	6p, 9q32–34, 18q21	None
16	Lachrymal glands, orbital soft tissue	None	None	3p14–21, 6p, 7p22, 8q24	None
17	Lachrymal glands	None	None	7p22, 8q24	None
18	Lachrymal glands	None	None	5q35, 8q24	None
19	Orbital soft tissue	None	Hepatitis C	8q24, 9q33–34, 11q12–13	None
20	Lachrymal glands	None	None	9q33–34, 11q12–13	None
21	Orbital soft tissue	None	CPS	5q35, 7p22, 7q22, 8q24, 9q34	None
22	Orbital soft tissue	None	CPS	8p21, 8q24, 11q12–13	None
23	Orbital soft tissue	None	None	1p32–36, 1p21–q23, 8q24, 11q12–13	None
24	Lachrymal glands	None	Hypothyroidism	3p21, 12	None
25	Conjunctiva	None	None	5q23, 9q33–34	None
26	Ocular adnexa (NS)	None	None	9q33–34, 18q12–23	None
27	Lachrymal glands	None	CPN	None	None
28	Orbital soft tissue	None	None	6p, 8p21, 8q24	6q12–14, 6q16/24
29	Lachrymal glands	None	HSV1/2	None	9q33
30	Ocular adnexa (NS)	None	ADV8	3, 6p, 8q24, 12q24, 18	None
31	Orbital soft tissue	None	CPS	None	1p32, 6q23
32	Orbital soft tissue	None	Previous sarcoidosis	1p12, 9q34, 12q24	1p36, 1q41, 1q31, 2p24–25, 4q32–34
33	Conjunctiva	None	None	3p21, 8q24, 9q34, 18	9q33

[a] Herpes simplex virus and adenovirus status were available in cases 25–33 from a previous study [16].
[b] Single BAC clone changes were included only if they were confirmed by tile-path array or fluorescence *in situ* hybridization.
[c] 6p gain was associated with trisomy 3: 4/8 (50%) cases with 6p gain had a trisomy 3, while only 3/25 (12%) cases without 6p gain had trisomy 3 ($p = 0.042$).
NS, not specified; CPS, *Chlamydia psittaci*; CTR, *C. trachomatis*; CPN, *C. pneumoniae*; HSV, herpes simplex virus; ADV, adenovirus.

J Pathol 2009; **217**: 420–430 DOI: 10.1002/path

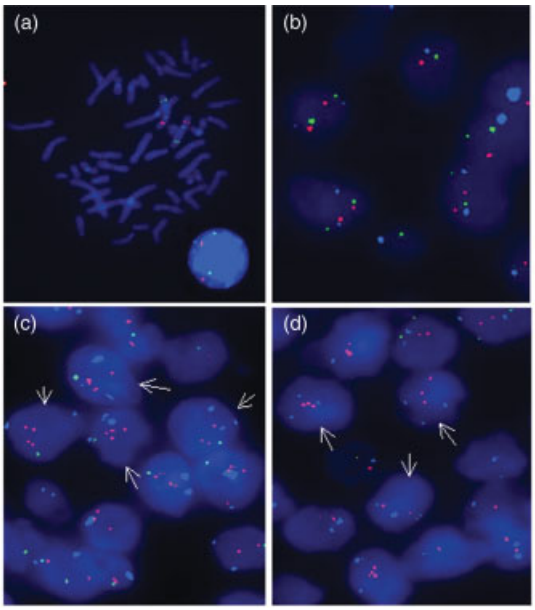

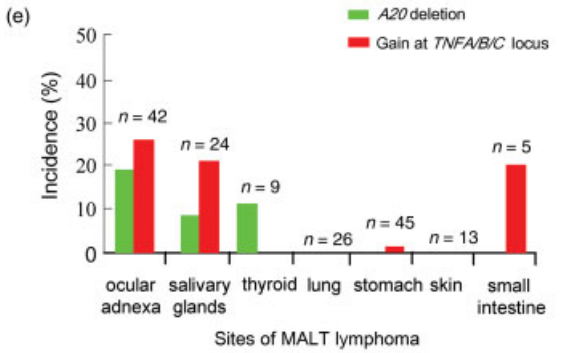

(f)

Number of cases	With *A20* deletion*	Without *A20* deletion#	Total
With gain at *TNFA/B/C* locus*	6	13	19
Without gain at *TNFA/B/C* locus#	6	141	147
Total	12	154	166

Figure 2. A20 deletion and *TNFA/B/C* gain in MALT lymphoma of various sites. (a–d) Three-colour FISH assay for investigation of copy number changes at the *A20* (RP11-356i2 labelled with spectrum green) and *TNFA/B/C* (bPG296P20 labelled with spectrum orange) loci, together with centromeric probe CEP 6 (spectrum aqua); cell nuclei showing chromosome 6 abnormalities are indicated by arrows. (a) Validation of FISH probes on metaphase spreads. (b) Ocular adnexal MALT lymphoma case 32 without evidence of chromosome 6 genetic abnormalities by high-resolution tile-path array–CGH. (c) Ocular adnexal MALT lymphoma case 28, showing *A20* heterozygous deletion, four copies of the *TNFA/B/C* and three copies of CEP6 probe signals. (d) Ocular adnexal MALT lymphoma case 12, showing A20 homozygous deletion and gain of an extra copy of the *TNFA/B/C* and CEP6 probe signals. (e) Incidence of *A20* deletion and *TNFA/B/C* gain in MALT lymphomas of various anatomical sites. Additionally, both *A20* deletion and *TNFA/B/C* gain have been found in one of the two hepatic MALT lymphomas. (f) Association between *A20* deletion and *TNFA/B/C* gain in MALT lymphomas of various anatomical sites ($p < 0.001$). **A20* deletion and gain at the *TNFA/B/C* locus were exclusively found in cases negative for MALT lymphoma-associated chromosomal translocations. #44% of the cases without chromosome 6 abnormalities had a MALT lymphoma-associated chromosomal translocation

relapses and the shortest relapse-free survival (case 2, Table 3).

There was no significant correlation between the presence of clinical features of autoimmunity and genomic abnormalities including *A20* deletion and *TNFA/B/C* locus gain. However, among the three cases with homozygous *A20* deletion, clinical data was available in two and both cases had an autoimmune disorder (Table 3).

In both ocular adnexal and pulmonary MALT lymphoma, there was no other apparent correlations among genomic abnormalities, evidence of *Chlamydia* infection, histological features, including plasma cell differentiation and extent of high-grade blast transformation, BCL10 staining pattern, age, sex, geographical origin, treatment and lymphoma relapse.

Discussion

The genomic profiles of 33 ocular adnexal MALT lymphomas and 25 pulmonary MALT lymphomas by 1 Mb array–CGH revealed both common and distinct recurrent chromosomal imbalances. Both MALT lymphomas of the ocular adnexa and lung showed frequent trisomies 3, 12 and 18 in t(11;18)(q21;q21)-negative cases and recurrent discrete gains at 8q24, 9q34 and 11q11–13, similar to the previous findings in gastric and salivary gland MALT lymphomas [13,14]. More importantly, we identified recurrent gains of chromosome 6/6p and deletion of 6q23 in ocular adnexal but not in pulmonary MALT lymphoma.

Deletion of 6q occurs frequently in a range of solid tumours and haematological malignancies [25–27]. Nevertheless, the regions of 6q deletion are relatively large and heterogeneous, and the genes targeted remain elusive [28]. In contrast, our study defined a MCR restricted to 1226 kb at 6q23.3. Bioinformatic search identified *A20* as the target of the deletion. While preparing our manuscript, Honma and colleagues demonstrated a similar diminutive deletion at 6q23.3–24.1 in six of 24 ocular adnexal MALT lymphoma cases and proposed *A20* as the deletion target [29,30]. *A20*, a potent inhibitor of NF-κB signalling, is required for termination of TNFα and TLR-induced NF-κB activation [21,22]. *A20* can specifically remove K63-linked polyubiquitin chains from TRAF6, a key molecule downstream of the CARMA1–BCL10–MALT1 complex in the NF-κB activation pathway [31]. A recent study shows that MALT1 and API2–MALT1 can proteolytically cleave *A20* [32], further implicating it in the molecular pathogenesis of MALT lymphoma.

By interphase FISH screening, we revealed that *A20* deletion occurred preferentially in MALT lymphoma of the ocular adnexa, salivary glands, thyroid and liver, but not in those of the lung, stomach, skin and small intestine. Importantly, *A20* homozygous deletion, hence complete inactivation of the gene, was seen in three of the 12 cases, suggesting that *A20* is likely a tumour suppresser gene. It remains to be investigated

Table 3. Demographic and clinico-pathological characteristics of MALT lymphomas with chromosome 6 abnormalities identified by interphase fluorescence *in situ* hybridization

Case[a]	Anatomical location	Stage at diagnosis	Sex	Age	Copy number by FISH			Autoimmune Disease	Treatment (response)	Follow-up period (months)	Lymphoma relapse	Outcome
					A20[b]	*TNFA/B/C* locus[c]	CEP6					
1	Orbital soft tissue	—	M	74	1	2	2	None	—	10	Axillary LN (10 m)	Alive with lymphoma
2	Orbital soft tissue, LG	1	F	60	1	2	2	None	RT (CR)	20	Preauricular and submandibular LN (8 m), soft tissue at neural foramen (16 m)	Alive with lymphoma
3	Orbital soft tissue, Conjunctiva	—	F	85	1	2	2	None	RT (CR)	33	None	Alive, no lymphoma
4	Orbital soft tissue	1	F	84	1	2	2	None	RT (CR)	12	None	Alive, no lymphoma
5	Orbital soft tissue, iliac LN	3	M	66	1	4	3[d]	None	RT (CR)	96	Submandibullar LN (72 m)	Alive, no lymphoma
6	Orbital soft tissue	1	F	63	1	3	2	None	RT (CR)	97	Scalene LN (12), opposite orbit (95 m), bone marrow (96 m)	Alive with lymphoma
7	Orbital soft tissue	—	—	—	1	3	3	—	—	—	—	—
8	Orbital soft tissue, LG, conjunctiva	—	F	84	0	3	3	Ulcerative colitis	—	—	—	—
9	Orbital soft tissue	1	M	51	2	3–4	2	None	Excision + RT (CR)	73	None	Alive, no lymphoma
10	Orbital soft tissue	1	M	78	2	3–4	3–4	None	RT (CR)	76	None	Alive, no lymphoma
11	Orbital soft tissue	1	M	68	2	4–5	2	None	RT (CR)	30	None	Alive, no lymphoma
12	Orbital soft tissue	1	M	64	2	4	3–4	None	RT (CR)	22	None	Alive, no lymphoma
13	Orbital soft tissue, LG	1	M	62	2	3–4	3[d]	None	NA (CR)	242	Opposite orbit (31 m)	Alive, no lymphoma
14	LG	1	F	60	2	3	2	None	RT (CR)	120	Submandibular LN (108 m)	Alive, no lymphoma
15	Ocular adnexa	—	F	71	2	4	3[d]	—	—	—	—	—
16	Salivary glands	—	F	44	0	2	2	Sjögren's syndrome, arthritis	—	36	Cervical LN (18 m), systemic follicular lymphoma[e] (24 m), bone marrow (36 m)	Alive with lymphoma
17	Salivary glands	—	M	6	1	3–4	2	—	—	—	—	—
18	Salivary glands	—	F	76	2	3	2	—	—	—	—	—
19	Salivary glands	—	F	64	2	3–4	3[d]	—	—	—	—	—
20	Salivary glands	—	—	—	2	3	2	Sjögren's syndrome	—	—	—	—
21	Salivary glands	—	M	40	3	3	3	—	—	—	—	—
22	Thyroid	—	F	62	1	2	2	—	—	—	—	—
23	Liver	—	M	66	0	3–4	3[d]	—	—	—	—	—
24	Small intestine, Mesenteric LN	—	F	46	2	4	2	—	—	—	—	—
25	Stomach	1	F	77	2	3	2	—	—	—	—	—

[a] With exception of case 9 (*FOXP1* with an unknown partner), all other cases are negative for translocations involving *MALT1, BCL10* and *FOXP1*. Cases 2–4 with *A20* deletion correspond to array–CGH cases 8, 13 and 31, respectively; cases 9–15 with gain at *TNFA/B/C* locus correspond to array–CGH cases 3, 5, 11, 15, 16, 29 and 30, respectively; cases 5 and 8 with both chromosome 6 abnormalities correspond to array–CGH cases 28 and 12, respectively, in Table 2.

[b] The abnormal *A20* probe signal (one copy or less) was found in >50% of nuclei in 9/12 (75%) cases (overall range, 17–94%; median, 52%).

[c] The abnormal *TNFA/B/C* probe signal (three copies or more) was in >50% of nuclei in 13/19 (68%)cases (overall range, 20–94%; median, 61%).

[d] Gains of only one extra copy of the centromeric probe 6 associated with two extra copies of the *TNFA/B/C* locus, suggesting the presence of an isochromosome 6p-6p [23].

[e] Follicular lymphoma is clonally linked to MALT lymphoma and both lymphomas harbour t(14;18)(q32;q21)/*IGH-BCL2* [24].

CEP, centromeric probe; — , unavailable; RT, radiotherapy; CR, complete response; m, months; LG, lachrymal glands; LN, lymph node.

J Pathol 2009; **217**: 420–430 DOI: 10.1002/path

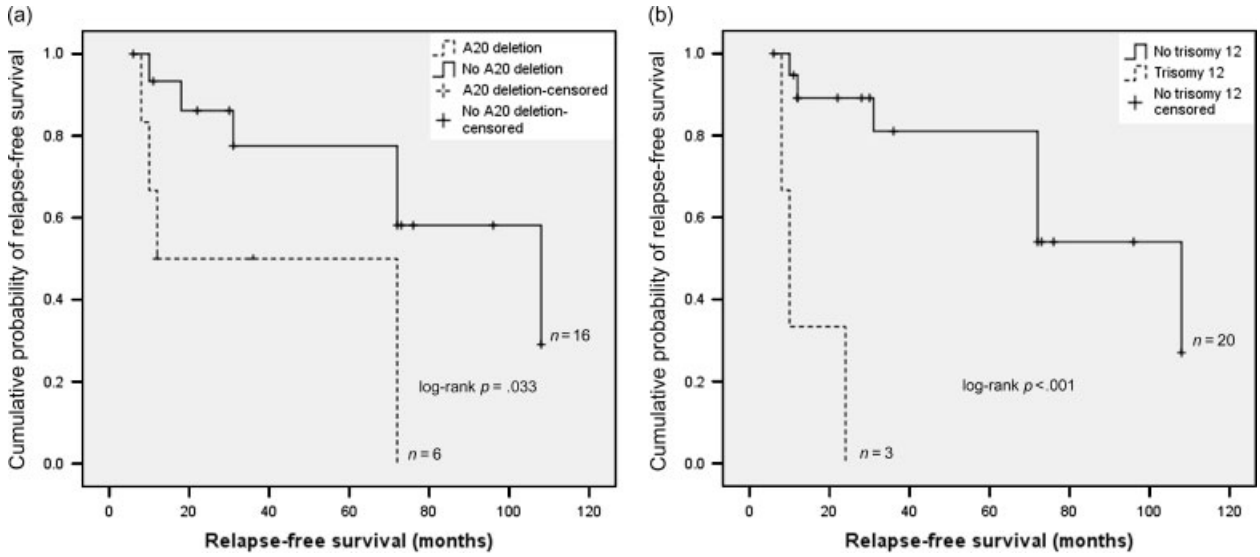

Figure 3. Relapse-free survival in ocular adnexal MALT lymphoma. Kaplan–Meier estimates with and without: (a) *A20* deletion; (b) trisomy 12. The lymphoma relapse-free survival was measured from the time of the diagnosis to the date of the first relapse. The event 'relapse' was right-censored

whether *A20* is also inactivated by somatic mutation and/or promoter methylation. Importantly, we also report for the first time evidence of an association between *A20* deletion and gain at the TNFA/B/C locus. High-resolution chromosome 6 tile-path array–CGH defined a 8.2 Mb MCR of gain at 6p21.2–22 and identified a novel recurrent focal peak within this MCR in four cases, which was centred at BAC clone bPG296p20 (6p21.33). Interphase FISH confirmed that this locus was further selected for extra copy gain, albeit at a moderate level, and showed that such gain was significantly associated with *A20* deletion. Among 15 genes within this BAC clone and its vicinity, *TNFA, TNFB, TNFC* and *NFκBIL1* are the most relevant in the context of lymphomagenesis. NFκBIL1, despite its name, does not function as an NF-κB inhibitor and may be involved in mRNA processing or translational regulation [33]. TNFA/B/C are powerful pro-inflammatory cytokines and potent activators of the NF-κB pathway [34]. The increased dosage of their genes may enhance their expression and thus NF-κB-activation. *A20* restricts TNF-induced NF-κB activities by inactivating and targeting the receptor interacting protein RIP, an essential mediator of TNF receptor signalling [35], for degradation through regulation of its ubiquitination [36]. A reduced *A20* gene dosage may impair such negative regulation and thus act synergistically with enhanced TNF receptor signalling.

The NF-κB activation pathway is commonly targeted by the oncogenic product of MALT lymphoma-associated translocations t(11;18)(21;q21)/*API2–MALT1*, t(1;14)(p22;q32)/*BCL10–IGH* and t(14;18)(q32;q21)/*IGH–MALT1* [8]. Our study revealed that *A20* deletion and *TNFA/B/C* gain occurred exclusively in MALT lymphomas without these translocations, providing evidence that genetic alterations in translocation negative MALT lymphoma also target the NF-κB pathway. Thus, a common molecular mechanism may be operational in these MALT lymphomas involving different oncogenic events.

A20 deletion was preferentially associated with MALT lymphoma of the ocular adnexa, salivary gland and thyroid. MALT lymphomas of the salivary gland and thyroid are closely associated with lymphoepithelial sialadenitis and Hashimoto thyroiditis, respectively [1]. There is evidence suggesting an association between autoimmunity and ocular adnexal MALT lymphoma, such as the involvement of the ocular adnexa by systemic lupus erythematosus and Sjögren's syndrome [37–38], frequent detection of serum rheumatoid factor in patients with ocular adnexal MALT lymphoma [39] and recurrent use of the autoimmune prone immunoglobulin heavy chain variable gene VH3-23 by the lymphoma cells [40]. TNF and TNF receptor signalling are critical to many immune responses and their deregulation is linked to several autoimmune disorders, including rheumatoid arthritis and systemic lupus erythematosus [41]. Recently, SNP genotyping shows that the *A20* gene locus is also associated with risk of rheumatoid arthritis [42] and systemic lupus erythematosus [43]. Clinical correlation in our series of ocular adnexal MALT lymphoma did not show significant correlation between *A20* deletion or *TNFA/B/C* locus gain and the presence of autoimmune disease, although two cases with homozygous *A20* deletion had an autoimmune disorder. The retrospective nature of our study may have underestimated the prevalence of autoimmunity in our patient cohort, and study of additional patients with clinical and laboratory evidence of autoimmunity is warranted.

A20 deletion and trisomy 12 were associated with adverse clinical parameters in ocular adnexal MALT lymphoma. *A20* deletion was significantly associated with lymphoma involvement of the orbital soft tissue

and with concurrent involvement of different adnexal tissues or distant spread at diagnosis. *A20* deletion was also more frequent in cases with lymphoma relapse than those without relapse and was significantly associated with a shorter lymphoma relapse-free survival. Similarly, trisomy 12 was significantly associated with both lymphoma relapse and a shorter lymphoma relapse-free survival. In view of the recent reports that a proportion of ocular adnexal MALT lymphoma is associated with *Chlamydia psittaci* infection and could be successfully treated by antibiotics [16,44], it is pertinent to investigate whether these genetic abnormalities impact on such treatment response and to prospectively validate the above clinical correlations in a large cohort of cases.

In summary, we identified NF-κB inhibitor *A20* as the target of 6q23 deletion in ocular adnexal MALT lymphoma and demonstrated that *A20* deletion was significantly associated with *TNFA/B/C* locus gain and occurred preferentially in translocation negative MALT lymphoma of the ocular adnexa and salivary glands, but not in those of the lung and stomach. *A20* deletion, associated with adverse clinical parameters in ocular adnexal MALT lymphoma, may play a critical role in the development of MALT lymphoma, particularly translocation-negative cases arising from sites involved by autoimmunity. Our study warrants further investigations to assess the potential link between *A20* deletion, *TNFA/B/C* gain, NF-κB activation, autoimmunity and the development of MALT lymphoma.

Acknowledgements

We thank Dr Paul Duthie, Christie Hospital NHS Foundation Trust, Dr Campidelli, University of Bologna, and Ms Sue Goddard, University College London, for their help in retrieving clinical data, as well as Dr Danita Pearson and Miss Alison Goatly for providing BAC clones and probe-labelling protocol for fluorescence *in situ* hybridization. The Du lab is supported by the Leukaemia and Lymphoma Society, the Elimination of Leukaemia fund, and Leukemia Research Fund. CB is supported by a Senior Clinician Scientist Fellowship from The Health Foundation, The Royal College of Pathologists and The Pathological Society of Great Britain and Ireland. The fluorescence microscope used in this study was funded by Cambridge Fund for the Prevention of Disease (CAMPOD), the Pathological Society of Great Britain and Ireland, and Openwork Foundation, Swindon. Array–CGH row data are available in the supporting information to this article.

Supporting information

Supporting information may be found in the online version of this article.

References

1. Du MQ. MALT lymphoma: recent advances in aetiology and molecular genetics. *J Clin Exp Hematop* 2007;**47:**31–42.
2. Ye H, Liu H, Attygalle A, Wotherspoon AC, Nicholson AG, Charlotte F, *et al*. Variable frequencies of t(11; 18)(q21; q21) in MALT lymphomas of different sites: significant association with CagA strains of *H. pylori* in gastric MALT lymphoma. *Blood* 2003;**102:**1012–1018.
3. Remstein ED, Dogan A, Einerson RR, Paternoster SF, Fink SR, Law M, *et al*. The incidence and anatomic site specificity of chromosomal translocations in primary extranodal marginal zone B-cell lymphoma of mucosa-associated lymphoid tissue (MALT lymphoma) in North America. *Am J Surg Pathol* 2006;**30:**1546–1553.
4. Ye H, Gong L, Liu H, Ruskone-Fourmestraux A, de Jong D, Pileri S, *et al*. Strong BCL10 nuclear expression identifies gastric MALT lymphomas that do not respond to *H. pylori* eradication. *Gut* 2006;**55:**137–138.
5. Goatly A, Bacon CM, Nakamura S, Ye H, Kim I, Brown PJ, *et al*. FOXP1 abnormalities in lymphoma: translocation breakpoint mapping reveals insights into deregulated transcriptional control. *Mod Pathol* 2008;**21:**902–911.
6. Haralambieva E, Adam P, Ventura R, Katzenberger T, Kalla J, Holler S, *et al*. Genetic rearrangement of FOXP1 is predominantly detected in a subset of diffuse large B-cell lymphomas with extranodal presentation. *Leukemia* 2006;**20:**1300–1303.
7. Hu H, Wang B, Borde M, Nardone J, Maika S, Allred L, *et al*. Foxp1 is an essential transcriptional regulator of B cell development. *Nat Immunol* 2006;**7:**819–826.
8. Isaacson PG, Du M.Q. MALT lymphoma: from morphology to molecules. *Nat Rev Cancer* 2004;**4:**644–653.
9. Liu H, Ruskone Fourmestraux A, Lavergne-Slove A, Ye H, Molina T, Bouhnik Y, *et al*. Resistance of t(11; 18) positive gastric mucosa-associated lymphoid tissue lymphoma to *Helicobacter pylori* eradication therapy. *Lancet* 2000;**357:**39–40.
10. Ye H, Gong L, Liu H, Ruskone-Fourmestraux A, de Jong D, Pileri S, *et al*. Strong BCL10 nuclear expression identifies gastric MALT lymphomas that do not respond to *H. pylori* eradication. *Gut* 2006;**55:**137–138.
11. Brynes RK, Almaguer PD, Leathery KE, McCourty A, Arber DA, Medeiros LJ, *et al*. Numerical cytogenetic abnormalities of chromosomes 3, 7, and 12 in marginal zone B-cell lymphomas. *Mod Pathol* 1996;**9:**995–1000.
12. Streubel B, Simonitsch-Klupp I, Mullauer L, Lamprecht A, Huber D, Siebert R, *et al*. Variable frequencies of MALT lymphoma-associated genetic aberrations in MALT lymphomas of different sites. *Leukemia* 2004;**18:**1722–1726.
13. Zhou Y, Ye H, Martin-Subero JI, Hamoudi R, Lu YJ, Wang R, *et al*. Distinct comparative genomic hybridization profiles in gastric mucosa-associated lymphoid tissue lymphomas with and without t(11; 18)(q21; q21). *Br J Haematol* 2006;**133:**35–42.
14. Zhou Y, Ye H, Martin-Subero JI, Gesk S, Hamoudi RA, Lu YJ, *et al*. The pattern of genomic gains in salivary gland MALT lymphomas. *Haematologica* 2007;**92:**921–927.
15. Johnson NA, Hamoudi RA, Ichimura K, Liu L, Pearson DM, Collins VP, *et al*. Application of array CGH on archival formalin-fixed paraffin-embedded tissues including small numbers of microdissected cells. *Lab Invest* 2006;**86:**968–978.
16. Chanudet E, Zhou Y, Bacon C, Wotherspoon A, Muller-Hermelink HK, Adam P, *et al*. *Chlamydia psittaci* is variably associated with ocular adnexal MALT lymphoma in different geographical regions. *J Pathol* 2006;**209:**344–351.
17. Ye H, Dogan A, Karran L, Willis TG, Chen L, Wlodarska I, *et al*. BCL10 expression in normal and neoplastic lymphoid tissue: nuclear localization in MALT lymphoma. *Am J Pathol* 2000;**157:**1147–1154.
18. Chanudet E, Adam P, Nicholson AG, Wotherspoon AC, Ranaldi R, Goteri G, *et al*. *Chlamydia* and *Mycoplasma* infections in pulmonary MALT lymphoma. *Br J Cancer* 2007;**97:**949–951.
19. McCabe MG, Ichimura K, Liu L, Plant K, Backlund LM, Pearson DM, *et al*. High-resolution array-based comparative genomic hybridization of medulloblastomas and supratentorial primitive neuroectodermal tumors. *J Neuropathol Exp Neurol* 2006;**65:**549–561.
20. Ichimura K, Mungall AJ, Fiegler H, Pearson DM, Dunham I, Carter NP, *et al*. Small regions of overlapping deletions on 6q26

in human astrocytic tumours identified using chromosome 6 tile path array–CGH. *Oncogene* 2006;**25:**1261–1271.
21. Boone DL, Turer EE, Lee EG, Ahmad RC, Wheeler MT, Tsui C, *et al*. The ubiquitin-modifying enzyme *A20* is required for termination of Toll-like receptor responses. *Nat Immunol* 2004;**5:**1052–1060.
22. Opipari AW Jr, Boguski MS, Dixit VM. The *A20* cDNA induced by tumor necrosis factor alpha encodes a novel type of zinc finger protein. *J Biol Chem* 1990;**265:**14705–14708.
23. Whang Peng J, Knutsen T, Jaffe E, Raffeld M, Zhao WP, Duffey P, *et al*. Cytogenetic study of two cases with lymphoma of mucosa-associated lymphoid tissue. *Cancer Genet Cytogenet* 1994;**77:**74–80.
24. Aiello A, Du MQ, Diss TC, Peng HZ, Pezzella F, Papini D, *et al*. Simultaneous phenotypically distinct but clonally identical mucosa-associated lymphoid tissue and follicular lymphoma in a patient with Sjogren's syndrome. *Blood* 1999;**94:**2247–2251.
25. Menasce LP, Orphanos V, Santibanez-Koref M, Boyle JM, Harrison CJ. Common region of deletion on the long arm of chromosome 6 in non-Hodgkin's lymphoma and acute lymphoblastic leukaemia. *Genes Chromosomes Cancer* 1994;**10:**286–288.
26. Ross CW, Ouillette PD, Saddler CM, Shedden KA, Malek SN. Comprehensive analysis of copy number and allele status identifies multiple chromosome defects underlying follicular lymphoma pathogenesis. *Clin Cancer Res* 2007;**13:**4777–4785.
27. Tagawa H, Suguro M, Tsuzuki S, Matsuo K, Karnan S, Ohshima K, *et al*. Comparison of genome profiles for identification of distinct subgroups of diffuse large B-cell lymphoma. *Blood* 2005;**106:**1770–1777.
28. Taborelli M, Tibiletti MG, Martin V, Pozzi B, Bertoni F, Capella C. Chromosome band 6q deletion pattern in malignant lymphomas. *Cancer Genet Cytogenet* 2006;**165:**106–113.
29. Kim WS, Honma K, Karnan S, Tagawa H, Kim YD, Oh YL, *et al*. Genome-wide array-based comparative genomic hybridization of ocular marginal zone B cell lymphoma: comparison with pulmonary and nodal marginal zone B cell lymphoma. *Genes Chromosomes Cancer* 2007;**46:**776–783.
30. Honma K, Tsuzuki S, Nakagawa M, Karnan S, Aizawa Y, Kim WS, *et al*. TNFAIP3 is the target gene of chromosome band 6q23.3-q24.1 loss in ocular adnexal marginal zone B cell lymphoma. *Genes Chromosomes Cancer* 2008;**47:**1–7.
31. Lin SC, Chung JY, Lamothe B, Rajashankar K, Lu M, Lo YC, *et al*. Molecular basis for the unique deubiquitinating activity of the NF-κB inhibitor *A20*. *J Mol Biol* 2008;**376:**526–540.
32. Coornaert B, Baens M, Heyninck K, Bekaert T, Haegman M, Staal J, *et al*. T cell antigen receptor stimulation induces MALT1 paracaspase-mediated cleavage of the NF0B inhibitor *A20*. *Nat Immunol* 2008;**9:**263–271.
33. Greetham D, Ellis CD, Mewar D, Fearon U, an Ultaigh SN, Veale DJ, *et al*. Functional characterization of NF-κB inhibitor-like protein 1 (NF-κBIL1), a candidate susceptibility gene for rheumatoid arthritis. *Hum Mol Genet* 2007;**16:**3027–3036.
34. Aggarwal BB. Signalling pathways of the TNF superfamily: a double-edged sword. *Nat Rev Immunol* 2003;**3:**745–756.
35. Kelliher MA, Grimm S, Ishida Y, Kuo F, Stanger BZ, Leder P. The death domain kinase RIP mediates the TNF-induced NF-κB signal. *Immunity* 1998;**8:**297–303.
36. Wertz IE, O'Rourke KM, Zhou H, Eby M, Aravind L, Seshagiri S, *et al*. De-ubiquitination and ubiquitin ligase domains of *A20* downregulate NF-κB signalling. *Nature* 2004;**430:**694–699.
37. Arevalo JF, Lowder CY, Muci-Mendoza R. Ocular manifestations of systemic lupus erythematosus. *Curr Opin Ophthalmol* 2002;**13:**404–410.
38. Bjerrum KB. Primary Sjogren's syndrome and keratoconjunctivitis sicca: diagnostic methods, frequency and social disease aspects. *Acta Ophthalmol Scand Suppl* 2000;**231:**1–37.
39. Kubota T, Moritani S, Yoshino T, Nagai H, Terasaki H. Ocular adnexal mucosa-associated lymphoid tissue lymphoma with polyclonal hypergammaglobulinemia. *Am J Ophthalmol* 2008;**145:**941–950.
40. Adam P, Haralambieva E, Hartmann M, Mao Z, Ott G, Rosenwald A. Rare occurrence of IgVH gene translocations and restricted IgVH gene repertoire in ocular MALT-type lymphoma. *Haematologica* 2008;**93:**319–320.
41. Mackay F, Kalled SL. TNF ligands and receptors in autoimmunity: an update. *Curr Opin Immunol* 2002;**14:**783–790.
42. Plenge RM, Cotsapas C, Davies L, Price AL, de Bakker PI, Maller J, *et al*. Two independent alleles at 6q23 associated with risk of rheumatoid arthritis. *Nat Genet* 2007;**39:**1477–1482.
43. Musone SL, Taylor KE, Lu TT, Nititham J, Ferreira RC, Ortmann W, *et al*. Multiple polymorphisms in the *TNFAIP3* region are independently associated with systemic lupus erythematosus. *Nat Genet* 2007;**39:**1477–1482.
44. Ferreri AJ, Ponzoni M, Guidoboni M, De Conciliis C, Resti AG, Mazzi B, *et al*. Regression of ocular adnexal lymphoma after *Chlamydia psittaci*-eradicating antibiotic therapy. *J Clin Oncol* 2005;**23:**5067–5073.